



ELSEVIER

Contents lists available at [SciVerse ScienceDirect](http://www.sciencedirect.com)

Comptes Rendus Physique

www.sciencedirect.com

Physics in High Magnetic Fields / Physique en champ magnétique intense

Optical spectroscopy on semiconductor quantum dots in high magnetic fields

*Spectroscopie optique de boîtes quantiques semiconductrices sous champs magnétiques intenses*Adam Babinski^a, Marek Potemski^b, Peter C.M. Christianen^{c,*}^a Institute of Experimental Physics, Faculty of Physics, University of Warsaw, Hoza 69, 00-681 Warszawa, Poland^b Laboratoire National des Champs Magnétiques Intenses, CNRS-UJF-UPS-INSA, B.P. 166, 38042 Grenoble Cedex 9, France^c High Field Magnet Laboratory, Institute for Molecules and Materials, Radboud University Nijmegen, Toernooiveld 7, 6525 ED Nijmegen, The Netherlands

ARTICLE INFO

Article history:

Available online 11 January 2013

Keywords:

Quantum dots
Optical spectroscopy
Magnetic fields

Mots-clés:

Boîtes quantiques
Spectroscopie optique
Champs magnétiques

ABSTRACT

We review the recent literature on the use of optical spectroscopy of semiconductor quantum dots in high magnetic fields. We address both self-assembled epitaxial dots and colloidal nanocrystal quantum dots, each of which has its own characteristic optical response. Combining simple theoretical models for quantum confinement with the effect of high magnetic fields we describe the basic optically allowed transitions expected for epitaxial and colloidal quantum dots. Within these models we discuss the effects of quantum confinement and orbital and spin Zeeman effects on the optical spectra, illustrated by experimental examples. Finally, effects of electron–electron and exchange interactions are addressed.

© 2012 Académie des sciences. Published by Elsevier Masson SAS. All rights reserved.

R É S U M É

Nous discutons l'application des méthodes de spectroscopie optique en champs magnétiques intenses aux études des boîtes quantiques semiconductrices, telles qu'elles sont présentées dans la littérature la plus récente. Nous traitons à la fois le cas des boîtes épitaxiales, auto-assemblées, et le cas des boîtes quantiques obtenues à partir de nano-cristaux colloïdaux. En combinant des modèles théoriques simples, concernant le confinement quantique, avec les effets de champ magnétique forte, nous décrivons les transitions optiques fondamentales qui sont attendues dans le cas de boîtes quantiques épitaxiales et colloïdales. Dans le cadre de ces modèles, nous discutons des conséquences sur le spectre optique des effets de confinement quantique et des effets Zeeman orbitaux et de spins, ce que nous illustrons à l'aide des exemples expérimentaux. Enfin, nous terminons en traitant le problème des effets électrons–électrons et d'interaction d'échange.

© 2012 Académie des sciences. Published by Elsevier Masson SAS. All rights reserved.

* Corresponding author.

E-mail addresses: babinski@fuw.edu.pl (A. Babinski), marek.potemski@lncmi.cnrs.fr (M. Potemski), p.christianen@science.ru.nl (P.C.M. Christianen).

1. Introduction

Semiconductor quantum dots (QDs) are nano-scale objects in which carriers are confined to spatial dimensions comparable to their *de Broglie* wavelengths. This confinement gives rise to several interesting phenomena leading to both new fundamental physics at the nano-scale and new opportunities for technological applications. A high magnetic field B has proven to be an important research tool to study the properties of QDs, because it modifies both their single-particle (SP) energy level structure and the mutual interactions between confined carriers. In the high field limit the typical size of the carrier cyclotron orbit, characterized by the magnetic length $l_B = \sqrt{\hbar/eB}$, becomes comparable to the QD dimensions, resulting in an appreciable diamagnetic energy shift of the ground state. Furthermore, at high fields both orbital and spin Zeeman splittings become important. Diamagnetic and Zeeman energies compete with the confinement-, Coulomb- and exchange-interaction energies in the high field regime. This can lead to several effects which can be analyzed to reveal specific properties of QDs. Interband optical spectroscopy is a very useful method to investigate QDs, in particular because the optical selection rules provide a way to characterize all orbital and spin quantum numbers. In this paper we will give a brief overview of the recent literature in this research area, mostly focusing on optical experiments on QDs in magnetic fields in excess of 10 T. The paper is divided in two parts, describing respectively self-assembled epitaxial QDs and colloidal nanocrystal quantum dots (NQDs).

2. Epitaxial quantum dots

Self-assembled semiconductor QDs can be manufactured by epitaxial growth methods, such as molecular beam epitaxy (MBE) or metalorganic vapor phase epitaxy (MOVPE). To obtain epitaxial QDs, one grows a thin layer of one semiconductor on top of an other semiconductor (with a higher bandgap), to which it is not lattice-matched. As a result of the strain small islands are formed on top of a two-dimensional wetting layer (Stranski–Krastanow growth mode). The islands are overgrown subsequently by a layer of the high bandgap material, leading to the formation of buried QDs which confine carriers in all three directions. The quantum confinement is stronger in the growth direction (1–10 nm) than in the lateral direction (10–50 nm). The growth and processing of semiconductor nanostructures are highly advanced nowadays, which enables the fabrication of high quality QD materials of possible use in a broad range of applications within opto-electronics, spintronics and quantum-information technology.

2.1. Single-particle energy levels

The analysis of optical properties of self-assembled QDs usually starts with the harmonic approximation of the lateral confinement potential for both electrons and holes [1,2] (Fig. 1).

2.1.1. Electrons

For electrons with parabolic dispersion relations, the evolution of the electronic SP states confined in a harmonic potential, with characteristic energy $\Omega_{e,0}$, in the presence of magnetic field B normal to the dot plane, is given by the well-known Fock–Darwin energy spectrum (FD states) [3,4]:

$$\varepsilon_i^e = \hbar\Omega_+^e \left(n + \frac{1}{2} \right) + \hbar\Omega_-^e \left(m + \frac{1}{2} \right)$$

Here, $i = n, m$ are integer quantum numbers and the frequencies Ω_{\pm}^e are given by:

$$\Omega_{\pm}^e = \sqrt{\Omega_{e,0}^2 + \frac{1}{4}\Omega_{e,c}^2} \pm \frac{1}{2}\Omega_{e,c}$$

where $\Omega_{e,c} = \frac{eB}{m_e^*}$ is the cyclotron frequency and m_e^* is the electron effective mass. $L_e = n - m$ is the electron angular-momentum number that depends on n and m . In this formula spin is neglected. In zero magnetic field the subsequent SP levels degeneracies are equal to 1 ($L_e = 0$), 2 ($L_e = +1, -1$), 3 ($L_e = +2, 0, -2$), etc. In analogy to atomic physics, these SP energy levels are usually referred to as s -, p -, d -, f -states (levels at positive energy in Fig. 1). In perpendicular magnetic field the s -level undergoes a diamagnetic shift towards higher energies. The p -level degeneracy is removed by the magnetic field due to the orbital Zeeman interaction. As a result the two levels related to the different angular-momenta shift towards lower and higher energies with increasing B . The energy splitting between those SP levels equals the electron cyclotron energy. Similarly the d -shell splits in magnetic field into three components and so on.

2.1.2. Holes

To analyze the QD *interband* optical properties, besides the electron states, also the hole states should be considered. The upper valence band in quantum confined structures is split into heavy hole and light hole bands. In self-assembled QDs with a built-in strain the light hole states have substantially higher energy than the heavy hole states and, therefore, only the latter states are usually considered. Within this approximation, the SP hole spectrum may also be described within

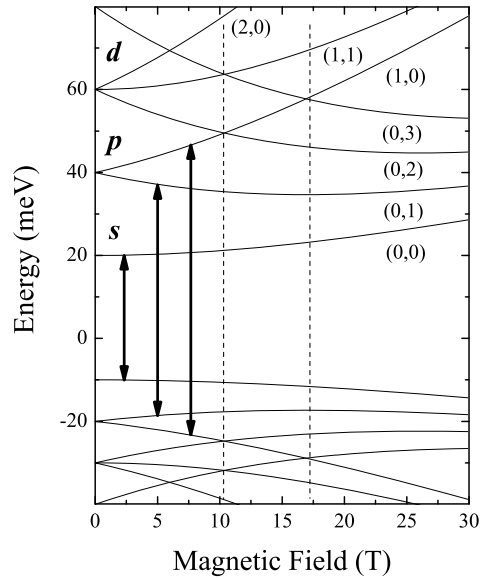


Fig. 1. Fock–Darwin spectrum: magnetic field evolution of single-particle electron and hole levels with harmonic lateral confinement of a characteristic energy $\Omega_{e,0} = 20$ meV (electrons) and $\Omega_{h,0} = 10$ meV (holes). The energy gap is taken zero ($E_g = 0$) and equal spatial extents of the electron and hole wavefunctions are assumed. The levels are labeled by the (n, m) quantum numbers (see text). The vertical arrows indicate dipole-allowed optical transitions for $N = 6$ electron–hole pairs. The dotted lines denote the magnetic fields at which the field-induced resonances of the SP states occur.

the harmonic potential model with characteristic frequency $\Omega_{h,0}$ (states at negative energy in Fig. 1). For dipole-allowed transitions, only electrons and holes with the same set of quantum numbers can recombine (see arrows in Fig. 1).

This simple model assuming a harmonic lateral potential results in energy shells in both the conduction and valence bands. As it will be shown later in this paper, this approximation holds well for example in the case of flat QDs grown by using the In-flush method [5]. The formation of electronic and hole energy shells in such QDs was confirmed by theoretical considerations [6], which also show a more complicated structure of the valence band in lens-shaped QDs.

2.2. Single excitons in high magnetic fields

Initial magneto-optical studies on QDs were focused on the diamagnetic shift of single electron–hole pairs (excitons). The magnetic field tends to squeeze wavefunctions of electrons and holes in a QD, which results in a diamagnetic shift of the exciton recombination energy. Thus, the excitonic diamagnetic shift of the excitonic emission is directly related to the spatial extent of the electron and hole wavefunctions. Because of the confinement this shift is significantly smaller for QDs than for bulk material for both directions of the magnetic field: parallel and perpendicular to the growth direction [7–9]. In fact the diamagnetic shift can be used to estimate the typical extension of the exciton wavefunction. Furthermore, the diamagnetic shift also depends on interparticle interactions and its detailed analysis must take into account the charge state of the QDs [10,11]. This leads to several effects: e.g. a negative diamagnetic shift reported for negatively charged excitons in small InAs/GaAs QDs [12]. In high magnetic fields the magnetic confinement becomes stronger than the geometrical one and the excitonic emission energy converges to the lowest Landau level of a two-dimensional electron–hole system with its characteristic linear field dependence. The deviation from the quadratic field dispersion was observed in several systems in both ensemble and single-dot experiments [13,14].

The Zeeman spin-splitting of single excitons was also investigated in a broad range of magnetic fields. The energy splitting of the neutral exciton in magnetic field results from the splitting of electron and hole energy levels in its initial configuration, i.e. before recombination. The Zeeman splitting of a negatively (positively) charged exciton is due to the hole (electron) level-splitting in the initial configuration and the electron (hole) level-splitting in the final state. In the first approximation, neglecting the small exchange-interaction splitting of the neutral exciton, both magnetic field dispersions should be identical and the Zeeman splitting should be a linear function of magnetic field [15]. Deviations from the linear dependence were however observed in single InAs/GaAs QDs [14], QDs formed in the InAs/GaAs wetting layer [16], and in both “bonding” and “antibonding” excitonic states in an InAs/GaAs QDs molecule [17]. The effect has been recently analyzed in more details by Jovanov et al. [18]. That nonlinearity is usually attributed to changes in the band mixing induced by the very high fields, as previously reported in structures of higher dimensionality as for example semiconductor quantum wells [19]. If the heavy hole–light hole mixing is not affected by the magnetic field one will obtain a linear Zeeman splitting, as usually observed in QDs at low fields [15]. If the band mixing is modified by the magnetic field, the Zeeman splitting would show a nonlinear dependence on magnetic field. Additionally, a nonzero envelope orbital momentum of holes was also proposed to account for a possible nonlinear Zeeman splitting of excitons in QDs in high magnetic fields [20]. It was

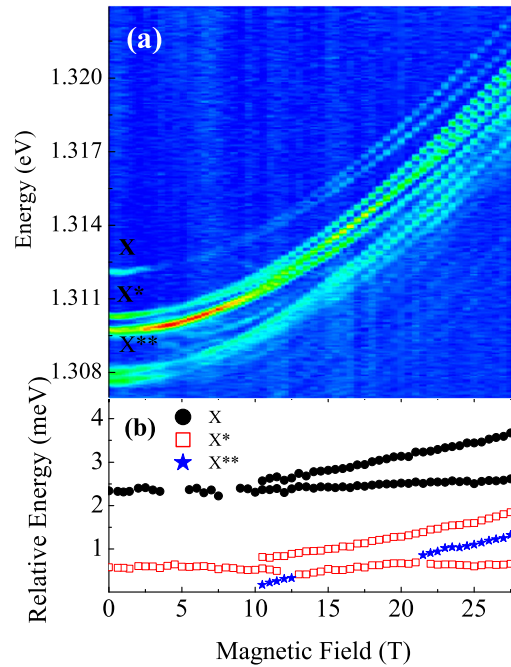


Fig. 2. (a) Photoluminescence related to the s -shell of a single InAs/GaAs QD in magnetic field up to 28 T. Emission lines related to the single neutral exciton (X), charged exciton (X^*) and doubly charged excitons (X^{**}) are seen. (b) Energy of the split emission lines relative to the lower-energy component of the X^{**} line.

shown that the spin and orbital motion of the hole state have opposite contributions to the hole g -factor, leading to zero g -factors of holes and then excitons in dots of a high aspect ratio. The theoretical model explained the strongly nonlinear splitting of excitons in flat, In-flashed InAs/GaAs QDs. The splitting was found to be close to zero in low magnetic fields and was observed to linearly depend on magnetic field in high field conditions (see Fig. 2) [14].

The photoluminescence excitation (PLE) spectrum of excitons in InAs/GaAs QDs was also investigated in high magnetic fields [21]. Application of magnetic field perpendicular to the plane of the QDs allowed to reveal the angular-momentum structure of the energy shells. The energy shell structure of a single exciton was found to follow the general FD pattern [3,4]. The blueshift of the PLE peaks with respect to the emission peaks was interpreted in terms of many-body interactions. It was shown that for a highly symmetric situation, the observed energy difference provided a direct measurement of the extra exchange energy gained upon addition of an extra exciton in the QD. In doped QDs excitation spectra are modified by a strong interaction of carriers in QDs with longitudinal optical phonons in the underlying semiconductor lattice. The resulting polarons, which are true excitations of a charged QD, were investigated in high magnetic fields by both far-infrared optical measurements probing intraband optical transitions [22,23] and PLE experiments, which give access to intraband transitions [24].

A completely different picture of the excitonic emission emerges when the QD electronic states can interact with the QDs environment. The most spectacular example of such an interaction is a coherent hybridization of localized QDs states and extended continuum states [25]. These states are generated by the emission of a photon from a QD. In high magnetic field the emission energy due to a negatively charged exciton X^{-3} , composed of four electrons and one hole confined in a dot, develops a series of oscillations, which result from interaction of the QD state with Landau levels in the wetting layer.

High magnetic field spectroscopy was also employed to study the brightening of dark excitons in a single CdTe/ZnTe QD containing a single Mn^{2+} ion [26]. It was shown that the optical recombination of the dark exciton was allowed when the exciton state was coupled to an individual magnetic impurity (manganese ion). The radiative recombination of dark excitons was found to be efficient only when the exchange interaction with the magnetic ion is accompanied by the heavy hole–light hole mixing, related to the in-plane anisotropy of the QD.

2.3. Multiexcitonic emission from quantum dots in high magnetic field

Optically excited semiconductor QDs can confine several electron–hole pairs. This leads to formation of multiexcitonic droplets, which can also be viewed as “artificial atoms” [27,28]. The total energy of such complexes comprises the kinetic energy of carriers, the energy of Coulomb interactions and energy due to correlations of the carrier movements. A complex spectrum arises as a result of those interactions. However, if the kinetic energy dominates, the magnetic field evolution of multiexcitonic optical emission spectra should in general resemble the FD pattern of the QDs SP structure.

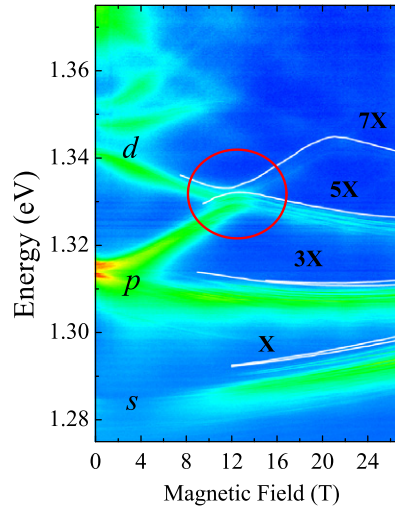


Fig. 3. Photoluminescence related to the s -, p -, and d -shells of a single InAs/GaAs QD in a magnetic field up to 27 T. Emission lines related to a single exciton (X), three excitons (3X), five excitons (5X) and seven excitons (7X) in a single QD are indicated by lines for clarity. The avoided level p_+ and d_- levels crossing is denoted by a red circle.

First optical measurements of multiexcitonic emission from QDs in magnetic field were limited to the low field range [29–31]. Substantial orbital Zeeman splitting of emission lines related to higher angular-momentum SP states was observed in emission from highly excited QDs induced by self-organized InP islands acting as stressors on InGaAs/GaAs quantum well [29,30]. The experimental results were quantitatively reproduced by calculations including the vertical quantum well-like confinement and the strain-induced, nearly parabolic, lateral confinement, together with the magnetic interaction. This approximate description of the data neglected the excitonic effects. The FD model of non-interacting carriers was also found to approximately explain the evolution of the emission from highly excited InAs/GaAs QDs by Paskov et al. [31]. The authors, however, also observed an excitation power dependence of the diamagnetic shift of the s -shell-related emission, which was explained in terms of the Coulomb-interaction screening in QDs.

The importance of excitonic effects for the energetic structure of multiexcitonic droplets was pointed out in high magnetic field optical measurements of highly excited self-assembled InAs/GaAs QDs in ensemble [32–34] and single-dot experiments [35,36] (see Fig. 3). Despite the qualitative resemblance of the investigated spectra to the FD pattern, clear deviations from the model were observed at magnetic fields where the crossings of the FD SP levels are expected to occur (see dashed lines in Fig. 1). The deviations were explained in terms of electron–electron interactions in multiexcitonic droplets. The interactions lead to a quasi-vanishing magnetic field dependence of the multiexcitonic emission energy near the crossing points as clearly evidenced in Fig. 3. Let us focus on the configurations of a five-exciton droplet in a QD. They are related to the p -shell $L_e = +1$ (p_+) and the d -shell $L_e = -2$ (d_-) levels before and after the SP level crossing respectively. The two configurations hybridize as they involve electron–hole pairs with zero total angular momentum. The energy of the multiexciton system averages over the energy of the two configurations with opposite magnetic field dependence leading to the observed effect of avoided level crossing (see Fig. 3). Moreover, neglecting higher shell scattering and assuming the same wavefunction for electrons and holes (hidden symmetry condition), for degenerate shells the chemical potential does not depend on the number of excitons and one obtains an exciton condensation effect [37].

The multiexcitonic energy structure of QDs was also shown to be affected by the spin–orbit coupling. Vachon et al. [38] observed at the top of the orbital splitting characteristic to the FD scheme, a doublet splitting of the multiexcitonic emission lines with unexpected magnetic field evolution. That behavior was explained in terms of the coupling of electron spin with the orbital angular-momentum envelope function. The effect of the spin–orbit coupling in the valence band was observed in polarization-sensitive PL measurements of highly excited InAs/GaAs QDs by Blokland et al. [39]. The pronounced circular polarization of the optical emission, together with the optical selection rules for orbital and spin quantum numbers, allowed to separate the individual electron and hole levels. Multiexcitonic droplets in large ensemble of InAs/GaAs quantum rings were also investigated by photoluminescence spectroscopy in high magnetic fields [40]. It was shown that the confinement of an electron and a hole in these type-I quantum rings along with the Coulomb interaction suppress the excitonic Aharonov–Bohm effect. In contrast the case of QDs with parabolic lateral confinement the multiexcitonic emission energies were found not to be equidistant. Moreover they split up to only two levels in magnetic field, which reflects the ringlike geometry of the confining potential.

3. Colloidal quantum dots

The optical properties of colloidal semiconductor nanocrystal quantum dots (NQDs) have attracted much interest over the recent years. In contrast to the self-assembled quantum dots discussed above, which are epitaxially grown, colloidal

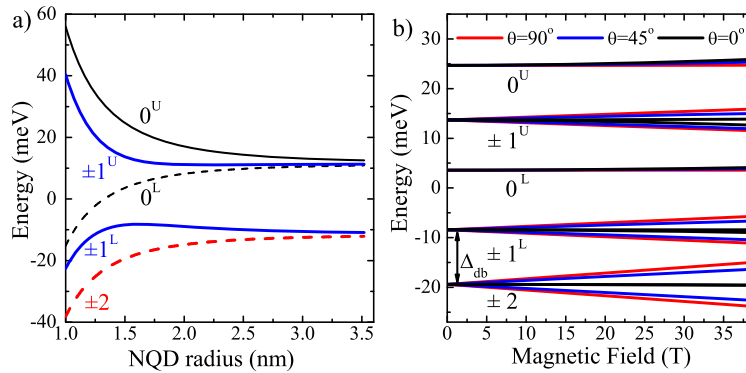


Fig. 4. (a) Calculated exciton fine-structure for a CdSe NQD as a function of size. The spectrum consists of five levels characterized by their spin projection (F_m) along the nanocrystal c -axis. With increasing energy: $F_m = \pm 2$, $F_m = \pm 1^L$, $F_m = 0^L$, $F_m = \pm 1^U$ and $F_m = 0^U$. (b) Calculated energies of the lowest exciton levels of a 1.5 nm radius CdSe NQD for several angles θ of the NQD c -axis relative to the field direction: $\theta = 90^\circ$ (red line), $\theta = 45^\circ$ (blue line) and $\theta = 0^\circ$ (black line).

nanocrystals are prepared relatively easy by using colloidal chemistry methods. These methods give easy control over the size and composition of the NQDs, including II–VI (CdSe, CdTe, ...) , III–V (InAs, InP, ...) and IV–VI (PbS, PbSe, PbTe) materials. It is, therefore, possible to tune the NQD exciton confinement energies, and thereby their emission wavelength, over a wide range [41–43]. This tunability combined with a high photoluminescence (PL) quantum efficiency of high quality NQDs, even at room temperature [44], make colloidal quantum dots very promising for novel applications [45], such as light emitting diodes [46–48], lasers [49,50], bio-labeling [51] and solar cells [52].

3.1. Exciton fine-structure of wurtzite NQDs

Three-dimensional confinement of electrons and holes in semiconductor NQDs leads to a discrete, atom-like level structure. In general the energy level structure of NQDs differs from that of their epitaxial counterparts. First of all, the typical NQD dimensions are in the 2–10 nm range, in all 3 directions, which is in most cases smaller than in epitaxial dots, resulting in larger effects of quantum confinement and exchange interactions. Because of these smaller dimensions higher magnetic fields are required to reach the regime where the magnetic length becomes comparable to the size of the NQDs. In general, the diamagnetic shift can, therefore, be safely neglected for colloidal dots in fields up to 60 T. Secondly, the prototypical example of a colloidal nanocrystals is a CdSe NQD [53,54], which has a wurtzite crystal structure with an extra crystal anisotropy that is absent in cubic zinc-blende structures. It is now well established that in wurtzite NQDs the electron-hole exchange interaction and the intrinsic crystal/shape anisotropy lift the spin degeneracy of the exciton levels, leading to five distinct states, characterized by their spin projection (F_m) along the nanocrystal c -axis (see Fig. 4a).

The resulting exciton fine-structure is characterized by a lowest energy exciton state ($F_m = \pm 2$), which is forbidden for direct radiative recombination, thus optically dark, and a higher-energy exciton state ($F_m = \pm 1^L$) that is dipole-allowed, thus optically bright. The separation between the two levels, denoted by the bright–dark splitting (Δ_{bd}), strongly depends on the NQD size because of the size-dependent exchange interaction. Evidence for this exciton fine-structure has been given by the dependence of the radiative lifetime on size [55–57] and temperature [58–60]. For typical values of Δ_{bd} of 5–20 meV only the lowest $|F_m| = 2$ level is populated at low temperatures ($k_B T < \Delta_{bd}$), leading to a relatively long exciton lifetime ($\approx 1 \mu\text{s}$) for a direct bandgap semiconductor material such as CdSe. However, with increasing temperature this lifetime strongly shortens when the higher $|F_m| = 1^L$ level becomes populated. Strong evidence for the dark nature of the exciton ground state of CdSe NQDs has been given by PL decay experiments in high magnetic fields [61,62]. In these experiments it was found that the exciton lifetime significantly decreases in an applied magnetic field, since the dark ground state acquires oscillator strength through field-induced mixing of the dark and bright exciton states. A typical example is given in Fig. 5a for a 2.1 nm CdSe NQD. This magnetic field-induced brightening is well described by Efros using an effective-mass model [53,54,61].

Further evidence for the exciton fine-structure has been given by fluorescence line narrowing (FLN) experiments [55,61, 63,64], in which PL is measured under resonant photo-excitation. Under non-resonant excitation the PL linewidth is rather broad (up to 100 meV) due to size-fluctuations of the NQDs. Under resonant excitation only NQDs that are resonant with the excitation wavelength will emit, leading to more narrow PL spectra exhibiting a clear structure (see Fig. 5b). Excitons are excited by the laser into the bright $|F_m| = 1$ level, which results in emission from the dark $|F_m| = 2$ excitons (zero-phonon line ZPL), several meV below the laser energy. Furthermore several phonon replicas (1PL, 2PL) are visible. In an applied magnetic field, using σ^+ polarized excitation and σ^- detection, the ZPL line shifts to lower energy due to the Zeeman splitting of the exciton levels. In addition the ZPL peak becomes more intense with field due to the increase of oscillator strength of the $|F_m| = 2$ level as a result of the exciton mixing, as discussed above. At high fields (> 15 T) an additional peak appears between the laser and the ZPL. This new peak is due to resonant σ^+ polarized excitation into the $F_m = +1^L$

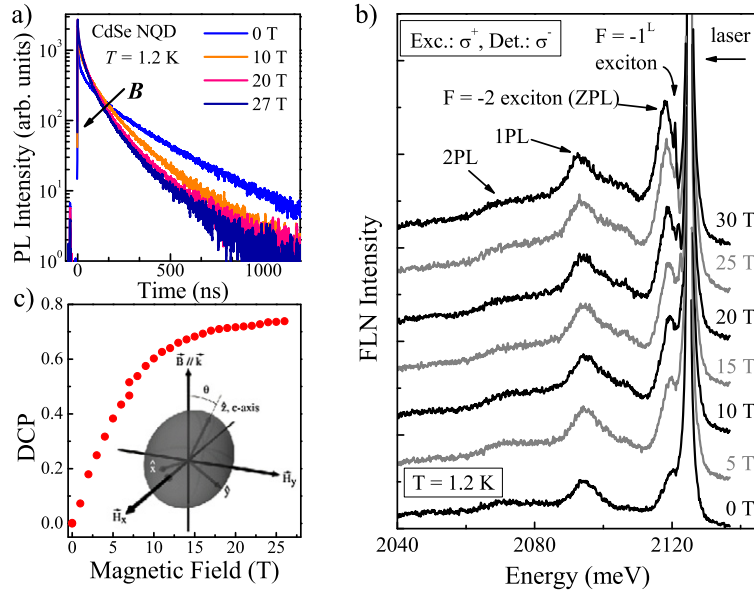


Fig. 5. Optical properties of a CdSe NQD. (a) Measured PL lifetime of a CdSe NQD with radius 2.1 nm at 1.2 K for several magnetic fields. (b) Fluorescence line narrowing spectra of a CdSe NQD at several magnetic fields. (c) Degree of circular polarization (DCP) of a CdSe NQD in an applied magnetic field at 1.2 K. Inset: the orientation of the NQD with angle θ of the crystal c -axis with respect to the polarization direction.

state and subsequent σ^- polarized emission of $F_m = -1^L$ excitons after a spin-flip process [63,64]. The measured splitting increases linearly with B and is directly related to the Zeeman splitting of the $|F_m| = 1^L$ levels.

The Zeeman splitting ΔE_Z of the exciton levels also leads to a pronounced circular polarization of the non-resonant PL. The degree of circular polarization is defined as $DCP = (I_{\sigma^-} - I_{\sigma^+}) / (I_{\sigma^-} + I_{\sigma^+})$ where I_{σ^\pm} is the PL intensity of the σ^\pm polarized emission. Typically the DCP increases linearly with field at low field strengths and saturates at high fields at a value of 0.5–0.75, considerably lower than the maximum DCP of 1 (see Fig. 5c). Remarkably, this saturation value is relatively insensitive to the temperature (when $k_B T < \Delta E_Z$) [62,64,65]. The saturation of the DCP thus has an intrinsic reason, which is related to the wurtzite structure of the CdSe NQDs [53,62,65–67]. The exciton emission strongly depends on the angle θ between the wurtzite c -axis and the direction of the magnetic field (see Fig. 4b and inset of Fig. 5c). The spin-splitting scales as $\Delta E_Z = g_{ex} \mu_B B \cos \theta$, with the exciton g -factor g_{ex} and the Bohr magneton μ_B . The PL intensities of the $F_m = +1^L$ and $F_m = -1^L$ levels are proportional to $P(\sigma^\pm) = (1 \pm \cos \theta)^2$ and $P(\sigma^\pm) = (1 \mp \cos \theta)^2$ respectively [53,66]. For the c -axis along the field ($\theta = 0^\circ$) the Zeeman splitting is maximal and the emission is fully circularly polarized. For this orientation there is no exciton mixing. In contrast, when the c -axis is perpendicular to the field ($\theta = 90^\circ$), the Zeeman splitting is zero, the emission is unpolarized and the exciton mixing is maximal. Averaging over all possible orientations of the NQDs within an ensemble experiment leads to a saturated DCP with a theoretically maximum value of 0.75, as observed in some experiments. Finite spin relaxation times [66] or the influence of non-radiative recombination [65] are possible origins for saturated DCP values lower than 0.75.

It is worth noticing that mixing of excitonic states, induced by application of strong magnetic fields is a relevant effect common for the physics of many other nanostructures. It largely helped us to understand the optical properties of carbon nanotubes [68,69] and to reveal some subtle physics of specific systems of semiconductor quantum dots with single magnetic atoms [26].

3.2. Different material systems

The PL wavelength of CdSe NQDs can be tuned across the visible wavelength region. Alternatively, zinc-blende (e.g. InAs, InP, CdTe, ZnS) and rock-salt (e.g. PbS, PbSe) NQDs have been fabricated, which have considerably enlarged the wavelength emission range [42,43]. From a fundamental point of view it is interesting to study NQDs with different crystal structures, since the lattice symmetry is one of the parameters to tune the lowest energy levels of the excitons that are responsible for the NQD optical properties [53,54,70]. To date, high magnetic field data are still scarce for NQDs with a crystal lattice different from wurtzite [67,71–74].

Surprisingly, the DCP of zinc-blende InP [67] and CdTe [75] and rock-salt PbS [73] has also been described by the formula that applies for wurtzite structures. So far a DCP approaching 1 has never been observed for semiconductor nanocrystals, which is most probably related to the fact that any shape anisotropy of the nanocrystals has an effect on the polarization properties that is similar to that of crystal anisotropy. The same conclusion has been drawn from recent experiments on the magnetic field dependence of the radiative lifetimes of excitons in zinc-blende CdTe NQDs. It was found that the exciton lifetime strongly decreases with increasing magnetic field, as well as with increasing temperature and size, similar to the

behavior of wurtzite CdSe NQDs. This is a remarkable result since spherical zinc-blende crystals with cubic symmetry have no crystal/shape anisotropy. The eight-fold degenerate exciton ground state is only split by the electron–hole exchange interaction, resulting in a five-fold degenerate, dark state, having $|F| = 2$ ($F_m = \pm 2, F_m = \pm 1^L, F_m = 0^L$) and a three-fold degenerate, bright state, having $|F| = 1$ ($F_m = \pm 1^U, F_m = 0^U$). The $|F| = 2$ and $|F| = 1$ states of such zinc-blende NQDs do not mix [53], resulting in an exciton ground state that should be dark at all magnetic fields, in contrast to the experimental results on CdTe NQDs. This discrepancy has been explained by taking into account a slight shape-asymmetry of the CdTe NQDs under study, because the theoretically predicted exciton fine-structure of prolate zinc-blende NQDs is similar to that of spherical wurtzite NQDs [74].

Evidence for an exciton fine-structure that is qualitatively different from that found in wurtzite NQDs has been recently reported for a rock-salt PbSe system [72]. By measuring the temperature-dependent PL decay times in magnetic fields up to 15 T it was found that the low temperature dynamics is determined by two, closely-spaced, exciton states with comparable, but small, oscillator strengths, in sharp contrast with the usual dark and bright states discussed above. Also in this system the PL decay time reduces with applied magnetic field due to field-induced mixing between the two states.

Apart from variation of the crystal structure of the NQDs to tailor their optical properties it is also feasible to vary the band alignment in hetero-nanocrystals. Here the NQDs consist of a core and a shell, and the band alignment can be designed to be type I or type II, a concept that is well known from epitaxial semiconductor nanostructures. In type-I structures the wavefunctions of the electrons and holes overlap, leading to spatially direct excitons. In type-II systems the electrons and holes are spatially separated leading to spatially indirect excitons. An intermediate case is given by so-called type-I^{1/2} or quasi-type-II structures, where one carrier is confined in the core and the second one is delocalized throughout the whole system [76]. A typical example is a CdTe/CdSe core/shell structure, for which it was shown that for a set of NQDs with fixed CdTe core and increasing CdSe shell thickness, the system gradually changes from type I to type II [76–78]. Reducing the overlap between the electron and hole wavefunctions, reduces the e–h exchange interaction and thus the dark–bright splitting, leading to strongly modified optical properties. This has been recently shown in a CdSe/CdS core/shell system, in which by increasing the shell thickness the bright–dark splitting was reduced to 0.1 meV, resulting in a material that emits with a nearly constant rate over temperatures from 1.5 to 300 K and magnetic fields up to 7 T. Importantly, this tunability is achieved for a nearly constant emission energy, which provides a new tool for controlling excitonic dynamics [79].

Magnetic doping of semiconductor nanostructures is a powerful method to boost and design their magnetic properties. In this respect, NQDs provide an excellent material platform given their flexibility and easy growth. Controlled incorporation of magnetic ions, such as Mn, has been demonstrated [80] and several new functionalities, such as a giant Zeeman splitting [81], light-induced magnetism [82] and modified optical properties [83,84] have been reported. In essence, this brings the magnetic response of NQDs into the low magnetic field regime, which is a prerequisite for novel applications in spintronics.

3.3. Magneto-optical spectroscopy on single NQDs

As described above optical studies of individual epitaxial quantum dots have given a wealth of new information on the properties of single neutral and charged excitons, as well as multiexcitonic complexes, since their Zeeman splitting and diamagnetic shift can be determined very accurately in the absence of ensemble averaging. Single-dot spectroscopy has also been performed quite extensively on NQDs, but results in magnetic fields are scarce and are restricted to CdSe systems and relatively low fields (<7 T) [63,85,86]. Magneto-PL results on single NQDs confirm that their magnetic response strongly depends on the angle of the *c*-axis with the applied field. The measured Zeeman splittings of the dark and bright exciton levels vary from dot to dot due to their different orientations. Furthermore, the field-induced exciton mixing could be directly observed in the PL spectra and decay of single CdSe NQDs. In this way the angle between the *c*-axis and the field can be determined for each NQD individually, as well as the *g*-factors for the bright and dark exciton states and the spin-flip relaxation rates between these levels [85,86]. Single NQD experiments also enable more detailed investigations of the excitonic energy spectrum. In analogy to the anisotropy observed in the *XY* plane of epitaxial dots (perpendicular to the growth (*Z*) axis), colloidal NQDs also exhibit such an anisotropy in the plane perpendicular to the *c*-axis [63,85,87]. Anisotropic energy splittings (Δ_{XY}) of the order of 1–3 meV have been reported. Magneto-PL on single CdSe NQDs reveal that NQDs with $\Delta_{XY} < 0.5$ meV demonstrate a conventional circularly polarized PL signal, whereas nanocrystals with large Δ_{XY} (>1 meV) show an anomalous magnetophotoluminescence polarization, wherein the lower-energy peak becomes circularly polarized with increasing field, while the higher-energy peak remains linearly polarized. This unusual behavior arises from strong mixing between the absorbing and emitting bright exciton levels due to the strong anisotropic exchange interactions [85,88].

References

- [1] R.J. Warburton, B.T. Miller, C.S. Dürr, C. Bödefeld, K. Karrai, J.P. Kotthaus, G. Medeiros-Ribeiro, P.M. Petroff, S. Huan, Phys. Rev. B 58 (1998) 16221.
- [2] A. Wojs, P. Hawrylak, Phys. Rev. B 55 (1997) 13066.
- [3] V. Fock, Z. Phys. 47 (1928) 446.
- [4] C.G. Darwin, Proc. Cambridge Philos. Soc. 27 (1930) 86.
- [5] Z.R. Wasilewski, S. Fafard, J.P. McCaffrey, J. Cryst. Growth 201 (1999) 1131.
- [6] M. Korkusinski, M. Zielinski, P. Hawrylak, J. Appl. Phys. 105 (2009) 122406.

- [7] P.D. Wang, J.L. Merz, S. Fafard, R. Leon, D. Leonard, G. Medeiros-Ribeiro, M. Oestreich, P.M. Petroff, K. Uchida, N. Miura, H. Akiyama, H. Sakaki, *Phys. Rev. B* 53 (1996) 16458.
- [8] R.K. Hayden, K. Uchida, N. Miura, A. Polimeni, S.T. Stoddart, M. Henini, L. Eaves, P.C. Main, *Physica B* 246–247 (1998) 93.
- [9] R.K. Hayden, K. Uchida, N. Miura, A. Polimeni, S.T. Stoddart, M. Henini, L. Eaves, P.C. Main, *Physica B* 249–251 (1998) 262.
- [10] C. Schulhauser, D. Haft, R.J. Warburton, K. Karrai, A.O. Govorov, A.V. Kalameitsev, A. Chaplik, W. Schoenfeld, J.M. Garcia, P.M. Petroff, *Phys. Rev. B* 66 (2002) 193303.
- [11] M. Korkusinski, P. Hawrylak, A. Babinski, M. Potemski, S. Raymond, Z. Wasilewski, *EPL* 79 (2007) 74005.
- [12] Y.J. Fu, S.D. Lin, M.F. Tsai, H. Lin, C.H. Lin, H.Y. Chou, S.J. Cheng, W.H. Chang, *Phys. Rev. B* 81 (2010) 113307.
- [13] A. Babinski, S. Avirothananon, J. Lapointe, Z. Wasilewski, S. Raymond, M. Potemski, *Physica E – Low-Dimens. Syst. & Nanostruct.* 26 (2005) 190.
- [14] A. Babinski, G. Ortner, S. Raymond, M. Potemski, M. Bayer, W. Sheng, P. Hawrylak, Z. Wasilewski, S. Fafard, A. Forchel, *Phys. Rev. B* 74 (2006) 075310.
- [15] A. Kuther, M. Bayer, A. Forchel, A. Gorbunov, V.B. Timofeev, F. Schäfer, J.P. Reithmaier, *Phys. Rev. B* 58 (1998) 7508.
- [16] A. Babinski, A. Golnik, J. Borysiuk, S. Kret, P. Kossacki, J.A. Gaj, S. Raymond, M. Potemski, Z.R. Wasilewski, *Phys. Status Solidi (b)* 246 (2009) 850.
- [17] G. Ortner, I. Yugova, G. Baldassarri Höger von Högersthal, A. Larionov, H. Kurtze, D.R. Yakovlev, M. Bayer, S. Fafard, Z. Wasilewski, P. Hawrylak, Y.B. Lyanda-Geller, T.L. Reinecke, A. Babinski, M. Potemski, V.B. Timofeev, A. Forchel, *Phys. Rev. B* 71 (2005) 125335.
- [18] V. Jovanov, T. Eissfeller, S. Kapfinger, E.C. Clark, F. Klotz, M. Bichler, J.G. Keizer, P.M. Koenraad, M.S. Brandt, G. Abstreiter, J.J. Finley, *Phys. Rev. B* 85 (2012) 165433.
- [19] N.J. Traynor, R.T. Harley, R.J. Warburton, *Phys. Rev. B* 51 (1995) 7361.
- [20] W. Sheng, A. Babinski, *Phys. Rev. B* 75 (2007) 033316.
- [21] S. Avirothananon, S. Raymond, S. Studenikin, M. Vachon, W. Render, A. Sachrajda, X. Wu, A. Babinski, M. Potemski, S. Fafard, S.J. Cheng, M. Korkusinski, P. Hawrylak, *Phys. Rev. B* 78 (2008) 235313.
- [22] V. Preisler, R. Ferreira, S. Hameau, L.A. de Vaulchier, Y. Guldner, M.L. Sadowski, A. Lemaître, *Phys. Rev. B* 72 (2005) 115309.
- [23] B.A. Carpenter, E.A. Zibik, M.L. Sadowski, L.R. Wilson, D.M. Whittaker, J.W. Cockburn, M.S. Skolnick, M. Potemski, M.J. Steer, M. Hopkinson, *Phys. Rev. B* 74 (2006) 161302(R).
- [24] V. Preisler, T. Grange, R. Ferreira, L.A. de Vaulchier, Y. Guldner, F.J. Teran, M. Potemski, A. Lemaître, *Phys. Rev. B* 73 (2006) 075320.
- [25] K. Karrai, R.J. Warburton, C. Schulhauser, A. Högele, B. Urbaszek, E.J. McGhee, A.O. Govorov, J.M. Garcia, B.D. Gerardot, P.M. Petroff, *Nature* 427 (2004) 135.
- [26] M. Goryca, P. Plochocka, T. Kazimierzczuk, P. Wojnar, G. Karczewski, J.A. Gaj, M. Potemski, P. Kossacki, *Phys. Rev. B* 82 (2010) 165323.
- [27] M. Bayer, O. Stern, P. Hawrylak, S. Fafard, A. Forchel, *Nature* 405 (2000) 923.
- [28] P. Hawrylak, *Phys. Rev. B* 60 (1999) 5597.
- [29] R. Rinaldi, P.V. Giugno, R. Cingolani, H. Lipsanen, M. Sopanen, J. Tulkki, J. Ahopelto, *Phys. Rev. Lett.* 77 (1996) 342.
- [30] R. Rinaldi, R. Mangino, R. Cingolani, H. Lipsanen, M. Sopanen, J. Tulkki, M. Brasken, J. Ahopelto, *Phys. Rev. B* 57 (1998) 9763.
- [31] P.P. Paskov, P.O. Holtz, B. Monemar, J.M. Garcia, W.V. Schoenfeld, P.M. Petroff, *Phys. Rev. B* 62 (2000) 7344.
- [32] S. Raymond, S. Studenikin, A. Sachrajda, Z. Wasilewski, S.J. Cheng, W. Sheng, P. Hawrylak, A. Babinski, M. Potemski, G. Ortner, M. Bayer, *Phys. Rev. Lett.* 92 (2004) 187402.
- [33] D. Smirnov, S. Raymond, S. Studenikin, A. Babinski, J. Leotin, P. Frings, M. Potemski, A. Sachrajda, *Physica B* 346–347 (2004) 432.
- [34] S. Avirothananon, W.D. Sheng, A. Babinski, S. Studenikin, S. Raymond, A. Sachrajda, M. Potemski, S. Fafard, G. Ortner, M. Bayer, *Jpn. J. Appl. Phys.* 43 (2004) 2088.
- [35] A. Babinski, M. Potemski, S. Raymond, J. Lapointe, Z.R. Wasilewski, *Phys. Rev. B* 74 (2006) 155301.
- [36] A. Babinski, M. Potemski, S. Raymond, J. Lapointe, Z.R. Wasilewski, *Phys. Status Solidi (c)* 3 (2006) 3748.
- [37] S.-J. Chen, W. Sheng, P. Hawrylak, *Phys. Rev. B* 68 (2003) 235330.
- [38] M. Vachon, S. Raymond, A. Babinski, J. Lapointe, Z. Wasilewski, M. Potemski, *Phys. Rev. B* 79 (2009) 165427.
- [39] J.H. Blokland, F.J.P. Wijnen, P.C.M. Christianen, U. Zeitler, J.C. Maan, P. Kailuweit, D. Reuter, A.D. Wieck, *Phys. Rev. B* 75 (2007) 233305.
- [40] N.A.J.M. Kleemans, J.H. Blokland, A.G. Taboada, H.C.M. van Genuchten, M. Bozkurt, V.M. Fomin, V.N. Gladilin, D. Granados, J.M. Garcia, P.C.M. Christianen, J.C. Maan, J.T. Devreese, P.M. Koenraad, *Phys. Rev. B* 80 (2009) 155318.
- [41] A.P. Alivisatos, *Science* 271 (1996) 933.
- [42] B.L. Wehrenberg, C. Wang, P. Guyot-Sionnest, *J. Phys. Chem. B* 106 (2002) 10634.
- [43] A. Shavel, N. Gaponik, A. Eychmuller, *J. Phys. Chem. B* 108 (2004) 5905.
- [44] L. Qu, X. Peng, *J. Am. Chem. Soc.* 124 (2002) 2049.
- [45] D.V. Talapin, J.-S. Lee, M.V. Kovalenko, E.V. Shevchenko, *Chem. Rev.* 110 (2010) 389.
- [46] V.L. Colvin, M.C. Schlamp, A.P. Alivisatos, *Nature* 370 (1994) 354.
- [47] S. Coe, W.-K. Woo, M. Bawendi, V. Mounsi, V. Bulovic, *Nature* 420 (2002) 800.
- [48] N. Tessler, V. Medvedev, M. Kazes, S. Kan, U. Banin, *Science* 295 (2002) 1506.
- [49] V.I. Klimov, A.A. Mikhailovsky, Su Xu, A. Malko, J.A. Hollingsworth, C.A. Leatherdale, H.-J. Eisler, M.G. Bawendi, *Science* 290 (2000) 314.
- [50] V.I. Klimov, S.A. Ivanov, J. Nanda, M. Achermann, I. Bezel, J.A. McGuire, A. Piryatinski, *Nature* 447 (2007) 441.
- [51] P. Alivisatos, *Nat. Biotechnol.* 22 (2004) 47.
- [52] A.J. Nozik, *Physica E – Low-Dimens. Syst. & Nanostruct.* 14 (2002) 115.
- [53] A.L. Efros, M. Rosen, M. Kuno, M. Nirmal, D.J. Norris, M. Bawendi, *Phys. Rev. B* 54 (1996) 4843.
- [54] A.L. Efros, M. Rosen, *Ann. Rev. Mater. Sci.* 30 (2000) 475.
- [55] D.J. Norris, A.L. Efros, M. Rosen, M.G. Bawendi, *Phys. Rev. B* 53 (1996) 16347.
- [56] S. Neeleshwar, C.L. Chen, C.B. Tsai, Y.Y. Chen, C.C. Chen, S.G. Shyu, M.S. Seehra, *Phys. Rev. B* 71 (2005) 201307.
- [57] C. de Mello Donegá, R. Koole, *J. Phys. Chem. C* 113 (2009) 6511.
- [58] S.A. Crooker, T. Barrick, J.A. Hollingsworth, V.I. Klimov, *Appl. Phys. Lett.* 82 (2003) 2793.
- [59] A.F. van Driel, G. Allan, C. Delerue, P. Lodahl, W.L. Vos, D. Vanmaekelbergh, *Phys. Rev. Lett.* 95 (2005) 236804.
- [60] C. de Mello Donegá, M. Bode, A. Meijerink, *Phys. Rev. B* 74 (2006) 085320.
- [61] M. Nirmal, D.J. Norris, M. Kuno, M.G. Bawendi, A.L. Efros, M. Rosen, *Phys. Rev. Lett.* 75 (1995) 3728.
- [62] M. Furis, J.A. Hollingsworth, V.I. Klimov, S.A. Crooker, *J. Phys. Chem. B* 109 (2005) 15332.
- [63] M. Furis, H. Htoon, M.A. Petruska, V.I. Klimov, T. Barrick, S.A. Crooker, *Phys. Rev. B* 73 (2006) 241313(R).
- [64] F.J.P. Wijnen, J.H. Blokland, P.T.K. Chin, P.C.M. Christianen, J.C. Maan, *Phys. Rev. B* 78 (2008) 235318.
- [65] E. Johnston-Halperin, D.D. Awschalom, S.A. Crooker, A.L. Efros, M. Rosen, X. Peng, A.P. Alivisatos, *Phys. Rev. B* 63 (2001) 205309.
- [66] M. Chamarro, C. Gourdon, P. Lavallard, *J. Lumin.* 70 (1996) 222.
- [67] L. Langof, L. Fradkin, E. Ehrenfreund, E. Lifshitz, O.I. Micic, A.J. Nozik, *Chem. Phys.* 297 (2004) 93.
- [68] J. Shaver, J. Kono, O. Portugall, V. Krstic, G.L.J.A. Rikken, Y. Miyauchi, S. Maruyama, V. Perebeinos, *Nano Lett.* 7 (2007) 1851.
- [69] A. Nish, R.J. Nicholas, C. Faugeras, Z. Bao, M. Potemski, *Phys. Rev. B* 78 (2008) 245413.
- [70] J.M. An, A. Franceschetti, A. Zunger, *Nano Lett.* 7 (2007) 2129.

- [71] L. Turyanska, U. Elfurawi, M. Li, M.W. Fay, N.R. Thomas, S. Mann, J.H. Blokland, P.C.M. Christianen, A. Patane, *Nanotechnology* 20 (2009) 315604.
- [72] R.D. Schaller, S.A. Crooker, D.A. Bussian, J.M. Pietryga, J. Joo, V.I. Klimov, *Phys. Rev. Lett.* 105 (2010) 067403.
- [73] L. Turyanska, J.H. Blokland, U. Elfurawi, O. Makarovskiy, P.C.M. Christianen, A. Patanè, *Phys. Rev. B* 82 (2010) 193302.
- [74] J.H. Blokland, V.I. Claessen, F.J.P. Wijnen, E. Groeneveld, C. de Mello Donega, D. Vanmaekelbergh, A. Meijerink, J.C. Maan, P.C.M. Christianen, *Phys. Rev. B* 83 (2011) 035304.
- [75] A. Granados del Aguila, E. Groeneveld, C. de Mello Donega, D. Vanmaekelbergh, A. Meijerink, J.C. Maan, P.C.M. Christianen, unpublished results.
- [76] C. de Mello Donegá, *Chem. Soc. Rev.* 40 (2011) 1512.
- [77] P.T.K. Chin, C. de Mello Donegá, S.S. van Bavel, S.C.J. Meskers, N.A.J.M. Sommerdijk, R.A.J. Janssen, *J. Am. Chem. Soc.* 129 (2007) 14880.
- [78] C. de Mello Donegá, *Phys. Rev. B* 81 (2010) 165303.
- [79] S. Brovelli, R.D. Schaller, S.A. Crooker, F. Garcia-Santamaria, Y. Chen, R. Viswanatha, J.A. Hollingsworth, H. Htoon, V.I. Klimov, *Nat. Commun.* 2 (2011) 280.
- [80] S.C. Erwin, L. Zu, M.I. Haftel, A.L. Efros, T.A. Kennedy, D.J. Norris, *Nature* 436 (2005) 91.
- [81] D.A. Bussian, S.A. Crooker, M. Yin, M. Brynda, A.L. Efros, V.I. Klimov, *Nat. Mater.* 8 (2009) 35.
- [82] R. Beaulac, L. Schneider, P.I. Archer, G. Bacher, D.R. Gamelin, *Science* 325 (2009) 973.
- [83] R. Beaulac, P.I. Archer, J. van Rijssel, A. Meijerink, D.R. Gamelin, *Nano Lett.* 8 (2008) 2949.
- [84] R. Viswanatha, J.M. Pietryga, V.I. Klimov, S.A. Crooker, *Phys. Rev. Lett.* 107 (2011) 067402.
- [85] H. Htoon, S.A. Crooker, M. Furis, S. Jeong, A.L. Efros, V.I. Klimov, *Phys. Rev. Lett.* 102 (2009) 017402.
- [86] L. Biadala, Y. Louyer, Ph. Tamarat, B. Lounis, *Phys. Rev. Lett.* 105 (2010) 157402.
- [87] H. Htoon, M. Furis, S.A. Crooker, S. Jeong, V.I. Klimov, *Phys. Rev. B* 77 (2008) 035328.
- [88] S.V. Goupalov, *Phys. Rev. B* 79 (2009) 233301.